Journal of Solar Energy Research (JSER)

Journal homepage: www.jser.ut.ac.ir

Implementation Investigation of Solar Energy Storage System Enhancement by Spiral-Finned Tube Heat Exchanger

Kadhim H. Suffer[a], Hiba A. Hasan[b], Vinous Majeed Hameed[c*], Malek Khalaf Albezuirat[d]

[a]*Mechanical Engineering Department, College of Engineering, Al-Nahrain University, Baghdad, Iraq*
[b]*College of Mechanical Engineering, University of Technology, Baghdad, Iraq*
[*c]*Chemical Engineering Department, College of Engineering, Al-Nahrain University, Baghdad, Iraq*
[d]*Department of Industrial Systems Engineering, Mutah University, Mutah, Alkarak 61710, Jordan*

ARTICLE INFO

Article Type:

Research Article

Received:2026.02.19
Accepted in revised form:2026.05.16

Keywords:

Solar energy;
CFD modelling;
PCM;
Latent heat storage;
Finned tube;
Solidification time

A B S T R A C T

This study verified paraffin wax as a phase change material (PCM), enhancing the performance of latent thermal energy storage. Computational Fluid Dynamics (CFD) software was used and validated by an experimental investigation to evaluate three vertical configurations of shell-and-tube heat exchangers: conventional (STHX), pin-finned (SFTHX), and a novel spiral wire-wound on pin fins (SSTHX).

Water at 20°C was fed through the tube to initiate PCM solidification**.** The CFD models' results showed significant outperformance of SSWTHX compared to other models. It showed a complete solidification process in 3193 seconds, while SFTHX exhibited 4317 seconds and STHX 5710 seconds. These results show a significant improvement in PCM thermal energy storage efficiency of 44% and 25% over STHX and STHX models compared to the SSWTHX model. Under 3000 seconds of the solidification process, 98% of paraffinic wax solidified in the SSWTHX-model compared to 90% in SFTHX. The increment in the SSWTHX surface area and the presence of the spiral wire in the heat exchanger resulted in the performance enhancement. The CFD temperature distribution showed strong agreement with the experimental work, which validated the three CFD models. These results supported the SSWTHX configuration with a higher thermal solar storage efficiency system.

[*]Corresponding Author Email: vinous.m.hameed@nahrainuniv.edu.iq

Cite this article: Suffer, K. , Hasan, H. , Hameed, V. M and Khalaf, M. (2026). Implementation Investigation of Solar Energy Storage System Enhancement by Spiral-Finned Tube Heat Exchanger. Journal of Solar Energy Research, 11(2), 2992-3009. doi: 10.22059/jser.2026.411357.1724

DOI: 10.22059/jser.2026.411357.1724

1. Introduction

The current technological development and the increasing demand for traditional fossil fuels have led to the depletion of these resources and rising economic costs. To obtain sustainable energy at lower costs, researchers have turned to various common, readily available renewable energy sources. The advantages of these sustainable energy sources are environmental friendliness and year-round availability. Numerous studies have demonstrated that researchers have successfully integrated various renewable energy sources to generate usable power for specific applications, thereby reducing the costs of traditional energy sources. Hashemian and Noorpoor (2023) [1] explored the possibility of combining solar and wind energy by proposing a hybrid system that combines wind power with a Rankine steam cycle to generate energy for heating and cooling applications, thereby reducing dependence on conventional energy sources. Solar energy is considered one of the most widely available renewable energies in most parts of the world. However, the main problem with utilizing solar energy is its availability during the day in sunny or partly sunny weather, while its unavailability during night or cloudy weather. Therefore, researchers have focused on storing the solar energy available during sunny weather for use during sunset. To store excess solar energy during the day, a heat exchanger is a common device used to exchange heat, and if its containing a phase-change material, that is helpful for storing absorbed heat from the solar energy. Some researchers have focused on developing different designs to improve the performance of heat exchangers used in such applications as Ismaeel et al. (2021) [2], who proposed a novel nozzle turbulator, which is used to enhance the heat exchanger performance. The concept of using phase-change materials (PCMs) in heat exchangers is to allow for heat storage during the melting (charging) phase and the recovery of this energy during the solidifying (discharging) phase. Therefore, it is quite possible to integrate such heat exchangers with solar collectors, a common system for harnessing solar energy for water heating, thereby improving collector efficiency. Numerous studies have focused on improving the thermal performance of solar energy systems through geometric optimization and enhancing the heat-absorbing surface. Abdel Latif et al. (2025) [3] found that the melting time of a phase-change heat storage material was reduced by using longitudinal fins, which improve heat transfer performance. Al-Yousifi and Ahmed (2025) [4] demonstrated the economic viability of solar thermal storage systems when combined with phase-change materials.

The utilization of a latent heat storage device (LHTE) has many benefits, such as its ability to provide thermal energy in large quantities, store energy for longer periods, and increase the system's efficiency. In thermal engineering, the heat transfer process can be optimized by adopting an appropriate heat exchanger. The main challenges facing latent thermal energy storage systems are the low thermal conductivity of the phase-change materials (PCMs) that are used in these systems. The idea of integrating thermal energy storage tanks (mostly heat exchangers) containing a phase-change material with a solar energy system has been very well accepted for storing solar energy that is available at the time when the sun is shining and utilizing it during sunset. Figure 1 shows how this idea is actually applied.

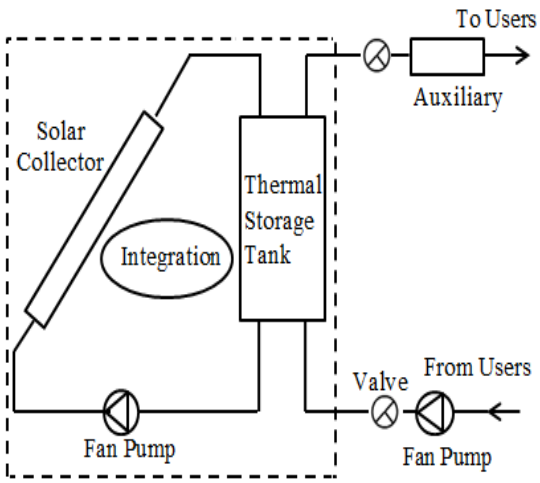

Figure 1. Integrated solar system with storage tank

Therefore, many studies have focused on transferring the heat as solar heat. For instance, Hasan and Jassim (2020) [5] investigated an experimental study for shifting the thermal energy in solar energy systems from day to night by using PCM to store the solar thermal energy and improve the thermal conductivity of these materials by enhancing heat transfer through the use of fins in different shapes. Daras Yazdanparast et al. (2026) [6] found that the presence of fins in single- and double-phase storage systems for PCMs demonstrated to improve the thermal conductivity and significantly enhance the melting rate of these materials under dependent solar heat flux. Similarly, Saleh et al. (2026) [7] demonstrated that thermal performance and heat transfer acceleration were enhanced by expanding the area for heat transfer and improving the thermal conductivity pathways through optimization of fin design in phase-change material (PCM)-based thermal systems. Other studies have shown that fin

geometries significantly affect the PCM change states. Alma' asfa et al. (2026) [8] demonstrated that different fin arrangements in a cylindrical system significantly impacted the melting dynamics of phase-change materials, as well as the temperature distribution. This causes an improvement in the overall efficiency and performance of thermal storage in solar systems. Another study deals with PCM melting and solidification processes through an innovative anchor fin design shell and tube ice storage units. The experimental study of this search shows that the solidification process is much faster than the melting point by 201.5%. Many variables in this article were studied, showing that the new fin design improved the melting by 1367.7% and 151.8% compared to a system with a longitudinal fin type [9]. [10] investigates the effect of tube shapes with the presence of fins on the solidification process of shell and tube heat exchangers. Three different tube shapes were selected (straight tube, nozzle, and reducer shapes). CFD software is used to predict different liquid fractions. The study proved that there is no significant effect on the variation of the liquid fraction. Solidification time is reduced by 25.7% with the nozzle shape model, while 16.3% is reduced with the reducer shape model compared to the normal tube shape. The nozzle model-shaped tube is preferred for the melting process. [11] reported a CFD simulation of PCM solidification in the finned heat pipes of a thermal energy storage system. In the same trend [12], in another study, both the charging and discharging times of a PCM were experimentally optimized in a heat exchanger with variable diameter annular fins to increase heat exchange between the fluid inside the tube and the surrounding PCM. The experimental results demonstrated that the exchanger's performance was improved by significantly reducing the charging and discharging times. Selected geometries, including a nozzle shape, shell-and-tube, and reducer with shell models, were studied by [13]. Their study indicates the required time for the PCM melt process, specifically paraffin wax, in a heat exchanger was (6130s) for the first model, (8210s) for the second, and (12,280s) for the third. The results also showed good agreement between the numerical simulations and experimental data. Different studies are carried out by [14, 15], which are interested in the cooling of a photovoltaic cell selected system using a phase change material (PCM) and a jetting method. The two studies were conducted using numerical simulations, followed by validation with experimental testing. The first study was conducted on four cases: a) using a phase change material with jetting, b) a phase change material without jetting, c) jetting without a PCM, and finally, d) without cooling. The second study focused on the experimental test with different jet diameters with that PCM. The results were acceptable, with a decrease in the temperature of the photovoltaic cells and an improvement in the performance and efficiency of the proposed system. [16] studied the feasibility of developing a solar collector type parabolic trough. Optimization processes were done by using three cases: the first case was using a copper tube with a corrugated outer surface to increase the surface area for absorbing heat from solar radiation. In the second case, PCM (paraffin wax) was used for the purpose of thermal storage. Their study results showed that the heat transfer rate increases by 40% for all selected volumetric flow rate ratios. The third case was to add a twisted copper ribbon inside the twisted tube, which improved the performance of the parabolic trough solar collector by 35%. Finally, their study concluded that the thermal efficiency increased by 85%. Since the thermal conductivity of thermal storage materials is low, some studies have focused on increasing the thermal storage efficiency by increasing the heat transfer area using different fin shapes. One such study, in [17], numerically investigated the use of Y-shaped fins and demonstrated their effect on the melting time in a solid-liquid system. The results of this study demonstrated that this fin shape led to a reduction in melting time. To verify these results, a comparison was made with data from a previous study. The results were satisfactory, finding that using fins enhanced the storage system with the PCM. Another study investigated the thermal performance of a compact heat exchanger system incorporating a latent heat storage system (LHTSS). The system consisted of a multi-tube heat exchanger with commercial paraffin wax RT44HC used as the energy storage medium. The study was conducted during both the melting and solidification processes. The findings indicated that heat transfer at the fluid inlet of the tubes significantly impacted the melting time compared to changes in the heat transfer rate resulting from variations in the fluid's volumetric flow rate. Increasing the volumetric flow rate reduced the phase change time. Furthermore, the melting time decreased with increasing temperature. The experimental results also demonstrated a longer required solidification time. Due to the low heat transfer coefficient of the phase change material (PCM), the solidification of the phase change material around the outer surface of the heat exchanger increased during the solidification process [18]. To enhance the storage ability, a numerical and experimentally study was carried out by [19] to investigate the time required for PCM (paraffin) melting processes for three proposed models; (STHX) the tradisional heat exchanger tube with shell, (SFTHX) model for adding pin fins to the

tradisional heat exchanger, while (SSWTHX) is the spiral wire winded around the pin fins with the traditional heat exchanger. Their results showed a significant improvement in thermal storage performance using the (SSWTHX) model, with a 37.5% increase in the charging time. For (SFTHX) model, the charging time was reduced by 21.3% compared to the conventional (STHX) model. Modi et al. [20] investigate the PCM thermal storage performance immersed in four longitudinal fin systems numerically. This study investigated many factors associated with the rig design factors, like angular position, fin height, and perforations with different hole sizes. This study shows that under the charging process, the temperature will rise, while the discharging process will not change. Also, the fin height has a positive effect on the charging process and does not show any effect through the solidification process. Finally, the effect of the perforation process, the study recommended a small hole diameter, which reduced the melting time by 12.65% compared to solid fins.

Through this narrative of the previous studies, most of these studies were about the possibility of exploiting and storing solar energy for use during times when the sun is not available. It becomes clear that there is still the possibility of applying ideas and modifications that can be used in developing and improving the performance of heat exchangers that are designed for solar thermal energy storage operations at the shortest available time to exploit solar energy in the event that is available for short times during the day. Therefore, the main research motivation for this study is to use two effective thermal enhancement techniques: phase change materials (PCM) that absorb and store the solar thermal energy through their melting process (charging case), and then the solidification process, which releases this stored heat in the PCM (discharge case). The main goal is to focus on the numerical simulations and experimental tests of the PCM (paraffin wax) solidification process, which will be applied to the three proposed models by [19] (STHX), (SFTHX), and (SSWTHX), where these models enhance the heat transfer rate due to the presence of spired-wire wound around pins, which increases the heat transfer surface area. The study tried to improve the thermal energy storage system and process thermal performance by enhancing the PCM discharge heat dissipation by applying these different types of heat exchangers. This study investigates the best heat exchanger configuration based on its thermal evaluation and PCM sodification, which represents the most utilized solar energy by applying the most effective heat exchanger fin configuration.

2. CFD Methodology and Physical Problems

2.1 Modelling of the Present Study Models

To achieve the objectives of this study, three models were created, with a three-dimensional model for the solar thermal energy storage system were modeled using SolidWorks 2018 software as presented in Figure 2. In Figure 2 (a), the first model was (STHX), the traditional heat exchanger (tube with shell). The tube is made from copper with an inside diameter of 16.4mm, while the PVC shell has 47.4 mm inside diameter. Figure 2 (b) shows a pin fin with a 1mm diameter and a length of 10.3 mm welded to the tube for the second proposed model (SFTHX), while in Figure 2 (c), the third proposed model was a spiral wire wound and welded on the tips of the fins (SSWTHX). The purpose of these modifications was to investigate numerically and experimentally the possibility of improving the solar thermal energy storage system performance to achieve the objective of this research in the solidification case by discharging the heat gained from solar energy that is stored in a phase change material (PCM) to heat the flowing water during a period after sunset and at night. The PCM used in these investigations is a paraffin wax with thermophysical properties tabulated in Table 1.

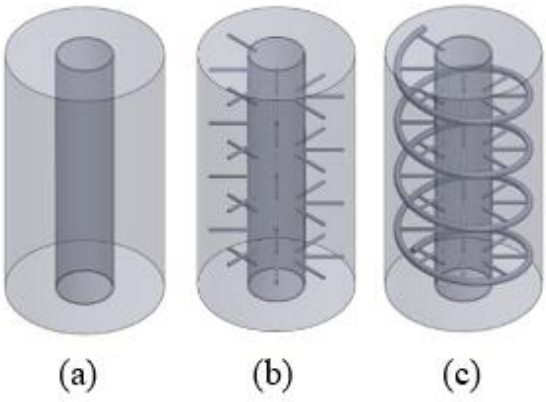

Figure 2. Modelling of (a) Shell and tube (STHX), (b) (SFTHX) adding pin fins to model (a) and (c) the spiral wire winded around the pin fins in model (b) (SSWTHX)

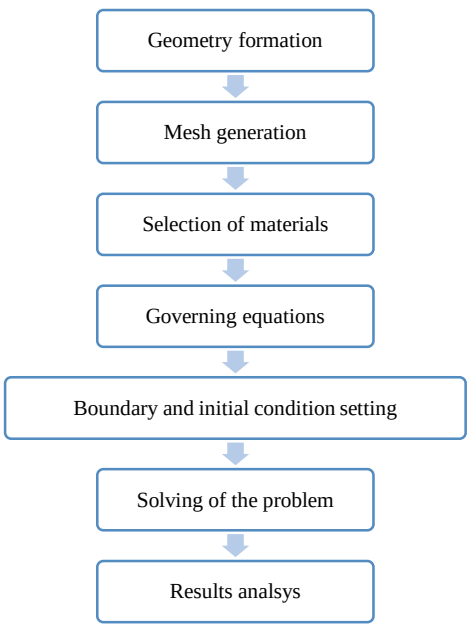

Figure 3. Flowchart of the methodology procedure

Table 1. Characteristics of Used Paraffin Wax (PCM) [19]	
Range of Melting Temperature	(326-340) K
Spesific Mass	850 kg/m3
Specific Heat Capacity	2817 J/kg·K
Coefficient of Viscosity	0.01215 kg/m·s
Latent Heat of Fusion	270715 J/kg
Thermal Conductivity	0.212 W/m·K
Coefficient of Heat Expansion	0.000305 1/K

To perform numerical simulations of the proposed models, all models prepared in SolidWorks 18 were exported to GAMBIT 2.4.6 for mesh generation and inclusion of boundary conditions. These models were then exported to ANSYS Fluent 19 [21] for numerical simulation and obtaining the desired results. The following steps were performed in Fluent software to complete the numerical simulation:

- Select the transient state and the time step.
- Melting and solidification models are activated for model specification, depending on the enthalpy porosity technique.
- Selecting materials, especially PCM, and determining all their properties.
- General governing equations are applied, and then a finite-volume method is used to solve the governing equations with a pressure-based solver, absolute velocity formulation, and a transient time
- For the solution steps (method), the selected scheme (SIMPLE) [22] (Patankar, 1980) was used for the pressure-velocity coupling. While for a segmentation of both energy and momentum governing equations, the upwind first-order is used.
- The hybrid initialization method is selected for the initialization of the solutions, and an initial temperature equal to its liquidus temperature is given to the PCM.
- Temperature and liquid fraction contours can be displayed as a result by using the Tecplot 360 programme, see Figure 3

For the mesh-independent models, the fluid fracturing parameter and tetrahedral mesh type were assumed and tested with different element sizes for each proposed model (STHX), (SFTHX), and (SSWTHX) separately, as shown in Figure 4. To ensure the accuracy of the results, different time steps of 0.25 s, 0.5 s, and 1.0 s were adopted. The SSWTHX model was chosen for the time step sensitivity analysis, as shown in Figure 4(a). For the subsequent simulations, a time step of 0.1 s was chosen based on the above evaluation. This provided a good balance between computational efficiency and numerical accuracy. In a further step, a mesh-independence study was also performed using different mesh densities, with the number of elements

being 1,145,585; 983,690; 586,339, and 418,899. Also, this study was presented using a 1.0-second time step, as shown in Figure 4(b). To ensure optimal accuracy while maintaining reasonable computational cost, a 0.8-mm mesh size was adopted for the tube, fin, and spirol coil components, while a 1-mm mesh size was used for the shell. The total number of resulting elements for the three heat exchanger configurations—STHX, SFTHX, and SSWTHX—was 919,423, 965,724, and 983,690, respectively. Figure 5 presents the SSWTHX model meshing (Tetrahedral). To ensure optimal accuracy and achieve the best computational cost, the best results were found at an element size of 0.8 mm for the tube model, while for the shell, a 1-mm mesh size is used. The total number of elements was found to be 919,423, 965,724, and 983,690 for STHX, SFTHX, and SSWTHX models, respectively. For the current simulation, a time step of 1 second was chosen to represent the time step with high sensitivity at different values. The PCM is also proposed to be at 324 K in the solid phase, while 373 K is assumed to be the constant temperature of the HTF wall. The outer surfaces of the structure are adiabatically insulated.

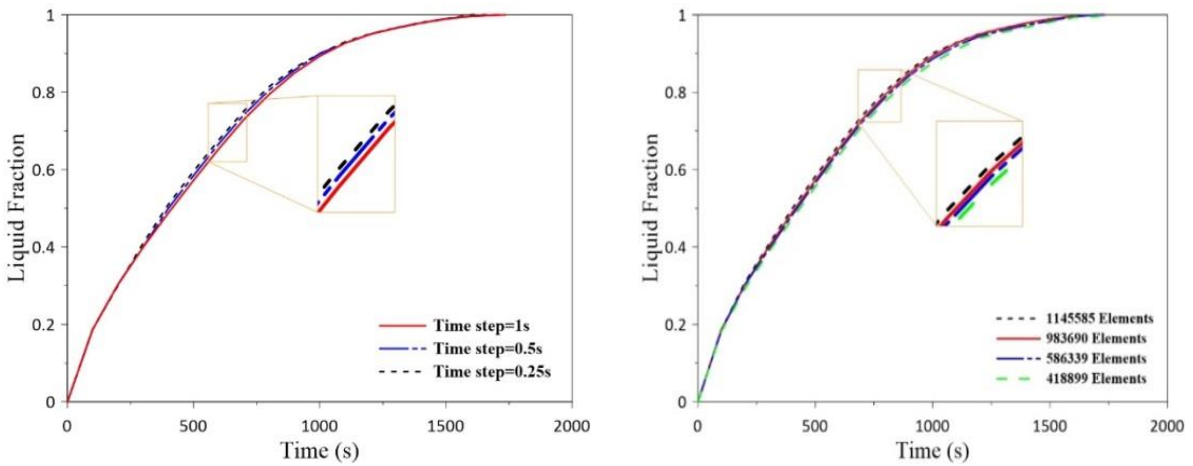

Figure 4. Variation of liquid fraction with time for the SSWTHX model. (a) Time step results, (b) Number of elements

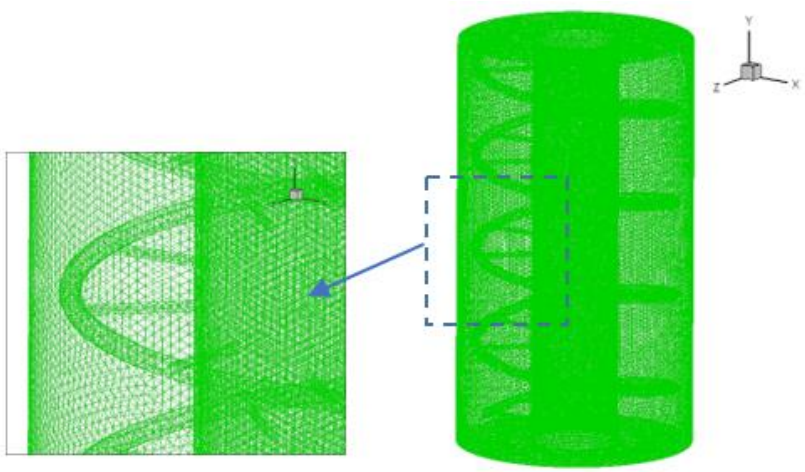

Figure 5. SSWTHX Model meshing (Tetrahedral)

2.2. Governing Equations

In this work, numerical simulation was conducted by applying the CFD technique with the method of the finite volume (FVM). Also, the Enthalpy – porosity technique was integrated with FVM, because of its wide recognition for its effectiveness in modeling phase change problems when using phase change materials (PCMs), which was originally introduced by [23].

It is worth noting that the phase transition zone—commonly indicated as the soft region, is a porous medium. Within this zone, the porosity is known as the fluid fraction, and its value ranges from 0 in the solid state to 1 when the material is completely molten [24]. The Boussinesq approximation [25] is applied when dealing with density changes resulting from temperature changes, assuming that the rest of the physical properties of the material remain constant during the phase change. Based on these assumptions, the numerical analysis model integrates both heat transfer and fluid flow dynamics in the molten zone, where buoyancy forces induce free flow. In the solidification process for the PCM liquid, the flow is considered unsteady, Newtonian for representing the natural convection, and laminar, and incompressible [26, 27]. Therefore, all governing equations are derived from the principles of mass continuity, momentum conservation, and energy conservation.

2.2.1 Assumptions to be Made for the Derivation of the Governing Equations

- Laminar, transient, and 3-D flow regime.
- Fluid is Newtonian and incompressible.
- All thermophysical properties are constant, except density in the buoyancy effect.
- The Boussinesq approximation is utilized for natural convection.
- Phase change process takes place through a mushy region employing the enthalpy-porosity approach.
- Liquid volume fraction increases linearly with respect to temperature during the phase change process.
- A thermal equilibrium state is established between the solid and liquid.
- Viscous dissipation effect is neglected.

Radiative heat transfer effect is neglected.
Equation of Continuity [28,29];

$$\frac{\partial \rho}{\partial t} + \nabla . \left(\rho \vec{V}\right) = 0 \qquad (1)$$

Equation of Momentum [30];

$$\rho \left(\frac{\partial \vec{V}}{\partial t} + \left(\nabla . \vec{V}\right)\vec{V}\right) = \mu\left(\nabla^2 \vec{V}\right) - \nabla P + \vec{S} \qquad (2)$$

Equation of Energy [26];

$$\frac{\partial}{\partial t}(\rho h) + \nabla . \left(\rho \vec{V} h\right) = \nabla . (K \nabla T) + S_h \qquad (3)$$

Where: t and V are time and velocity, μ and ρ are the viscosity and density of the phase change material, P and $\vec{s}$ are the global pressure and momentum sources, K is the conductivity, and h is the enthalpy. The momentum source is expressed in Equation (2) based on [31];

$$\vec{s} = \frac{(1-\beta)^2}{(\beta^3+)^3} A_{mush} \vec{V} \rho \vec{g} \gamma (T - T_0) \qquad (4)$$

t, V, μ, ρ, P, K, and $\vec{s}$, $\vec{g}$, γ, and T_0 are explained briefly in the nomenclature table. The momentum source is expressed in Equation (2) based on [31];
Where β is a fraction of solid was considered very small to avoid a zero value in the denominator. Amush is adjusted to a value of 105 kg/m3 to represent the (constant mesh region) applied according to both [32] and [33]

3. Experimental tests Setup

The schematic diagram of the assembly of the fabricated parts for the experimental test system is presented in Figure 6 (a). The experimental system consists of two baths (hot and cold) used for the purpose of conducting the paraffin melting and solidification processes. For proposed temperature measuring, two temperature controllers, two control valves, piping and flowmeter device has (±0.3%) accuracy, instrument data logger for measuring temperature with accuracy of (±0.06), three type-K thermocouples ± (0.4% + 1°C) accuracy inserted inside the test section, the first at the water inlet, and the second at the water outlet, and the third at the water flowing from the bottom to the top of the tested models. To ensure the accuracy of the experimental readings, all devices are checked at the zeroth point, and several readings are done to ensure the accuracy of this device's readings. The dimensions and other details are presented in Figure 6 (b) for the proposed models.
The models that are modeled for the numerical part are manufactured for conducting experiments and tests in order to compare and verify the numerical results. Figure 7 (a, b, and c) presents the manufacturing of three models (STHX), (SFTHX), and (SSWTHX), respectively. It appears that all three models are made from copper tube (1 mm) pin fins, a diameter of 10 mm, long, welded to the copper tube for the SFTHX model, and 2 mm diameter and 125.66

mm long of copper wire, and 40 mm diameter is wound spirally into four winds and welded with the pin fins tips to make the SSWTHX model. PVC shells with 50 mm outer diameter and 3 mm thickness are used with all models, as shown in Figure 8 (a). Paraffin is filled in the space between shells and models Figure 8 (b).

Three Type-K thermocouples are inserted into the PCM at a depth of 3 mm to measure the temperature during the melting and solidification processes.

Two thermocouples for measuring (T_{out} and T_{in}) are fixed near the beginning and exit of the flowing water inside the tube. Finally, a 10 mm thick rubber insulator was wrapped around all PVC sheaths for thermal insulation, as shown in Figure 8 (c). The main idea of fabricating the SSWTHX model is to increase the transfer of the stored heat in PCM that crosses the tube wall to the flowing fluid inside the tube. This reduces the required time for the discharge of the heat from the PCM and then improves the heat transfer in the solidification processes.

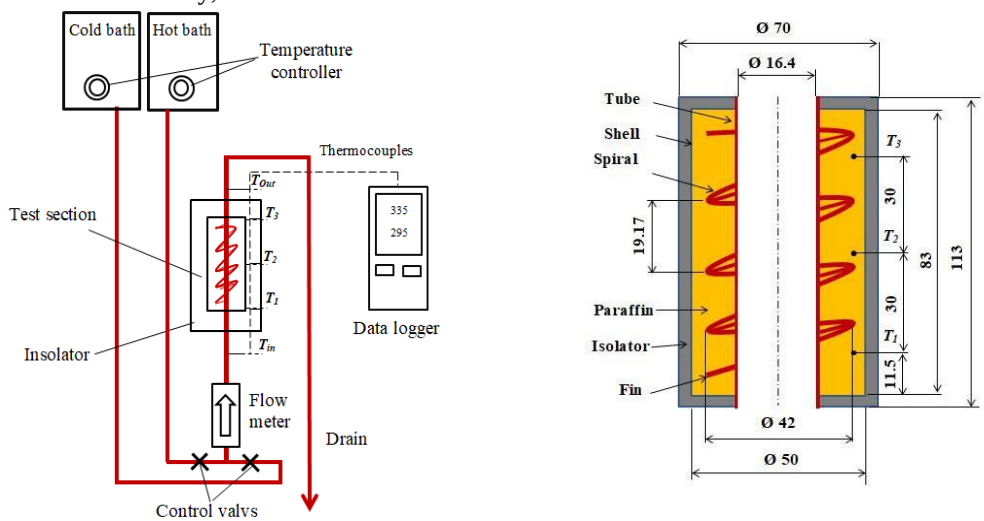

(a) (b)

Figure 6. Experimental test system of (a) Experimental set-up, (b) Test Section (dimensions in mm)

Figure 7. Fabricated tube configuration for the three models is: a- STHX, b-SFTHX, and c- SSWTHX

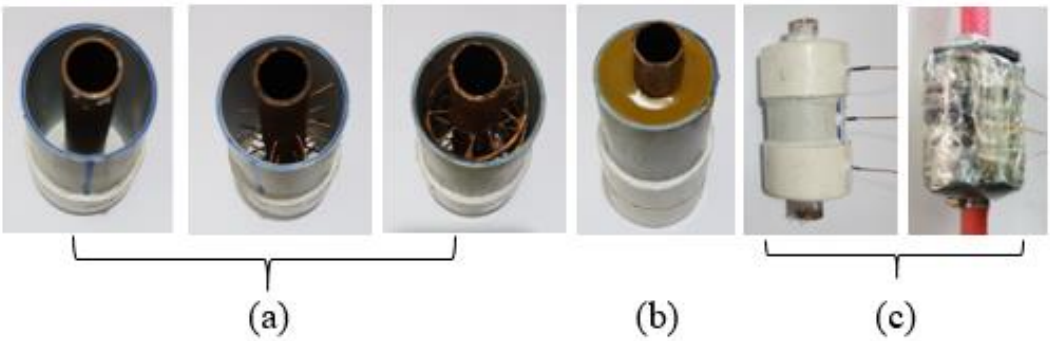

Figure 8. Photographs of the experimental setup include: (a) Tube with shell, Finned tube with shell, Spiral wire with shell, (b) Shell filled with paraffin, and (c) Thermocouples locations and insulator

4. Results and Discussions

In this study, numerical (CFD) simulations were carried out on the models. suggested Figure 2 shows the solidification (discharge) process of stored solar energy as latent heat in paraffin. It is assumed that the flowing fluid (water) enters the tube from the bottom at a temperature of 20°C in all models, then exits from the top. Also, the solidification process began when the paraffin was in a fully melted state. Figure 9 (a) presents the contour plot of the predicted solidification fraction in the STHX model, illustrating the progression of crystallization and solidification. It can be noted that the solidification layers grow over time around the tube for each model. The thickness of the solidification layer increases at the bottom and decreases at the top, forming a cone shape in the direction of the flowing liquid inside the tube. This occurs because the paraffin loses more heat at the beginning of the flow than at the exit of the tube. The solid layer began to increase gradually as noted at the times 500 (s), 1000 (s), and 2000 (s). When the processing time reaches 2000 (s), the paraffin has nearly discharged 75% of its stored energy to the flowing water. From the SFTHX model results, it was observed that the solidification process is significantly faster compared to the STHX model, as shown in Figure 9 (b). After 2000 (s) from starting solidification processes, 85% of the PCM is solidified, while when the time reaches 3000 (s), 90% of the paraffin has solidified. Figure 9 (c) shows the SSWTHX model, which exhibits the fastest solidification than the SFTHX and STHX models, as noted from the solidification times at 2000 (s), more than 95% of paraffin is changed to the solid. When time reaches 3000 (s), 98% of the paraffin has solidified, and it has released most of the stored latent heat energy to the flowing water. In contrast, the STHX model shows slower solidification dependent on the limited surface area for transferring heat. The STHX model shows slower solidification due to its limited heat transfer surface area. In contrast, the SSWTHX model exhibits faster solidification than the SFTHX and STHX models. Combining the spiral wire with pin fins ensures better heat distribution between the PCM and the flowing water, enhancing the heat transfer process. The presence of fins, whether pin-finned alone or with the spiral wire, improves the efficiency of heat transfer between the paraffin and the cooling fluid. The SSWTHX model, in particular, offers the best performance due to its superior distribution of heat transfer. This improvement is explained by the fact that the heat transfer surface area of the three models is: 4535, 5602.9, and 6124 mm^2 for STHX, SFTHX, and SSWTHX, respectively.

4.1 CFD Model Assumptions

- The temperature distribution is constant within the computational domain.
- No-slip wall boundary condition is considered at all solid boundaries.
- Insulated walls of the container, excluding heat exchanger walls.
- Constant temperature (or heat flux) at heat exchanger walls.
- Gravitational acceleration is perpendicular to the horizontal plane.
- Solid region is modeled as porous media with zero velocity.
- Mushy region flow is modeled with a Darcy damping term.
- No change in volume with phase transition.
- Pure system with no contamination and chemical reaction.
- A grid-independent mesh is used.

Figure 10 illustrates the average solid fraction of the paraffin during the solidification process. When the value is 0, it indicates that the state of paraffin is solidified, while when the value is 1, it means that the paraffin is still in the liquid phase. It is clearly shown in Figure 10 that the SSWTHX model is faster in solidification to reach the value 0 compared to the other models. The numerical simulation results indicate that at time 3193 (s), in the SSWTHX model, the PCM is observed to be fully solidified, while for both the SFTHX and STHX models, the time required to reach the solid phase is 4317 (s) and 5710 (s), respectively. From these results, it can be observed that 44% of paraffin solidification occurs in the SSWTHX model while 25% occurs in the SFTHX model. Therefore, these two models are considered faster in the paraffin solidification process compared to the STHX model. These results indicate that the proposed pin fins enhance heat transfer by increasing the surface area between the paraffin and circulating water, thereby accelerating the solidification of the paraffin. Similarly, the spiral wire enhances the heat transfer rate from the paraffin through conduction; the spiral shape also boosts convective heat transfer within the paraffin, further accelerating the solidification process. As a result, the overall heat transfer efficiency of the system is improved by the combined effects of the pin fins and the spiral wire.

Figure 11 shows the contours of the temperature distribution in the paraffin for the previous three suggested models of Figure 2. The temperature distribution in the SFTHX model shows that the pin fins create a more extended area and provide better distribution for transferring the latent heat available in the paraffin to the cooling liquid flowing inside the tube. From these contours, when the time reaches 2000 (s), it can be seen that the solidification process is more rapid in the SFHTX model compared to the STHX model. The last part of the contours of the temperature distribution inside the paraffin for the SSWTHX model shows that the winding of the spiral wire around the pin fins provides a better-extended area and good distribution; this helps to transfer the latent heat from the paraffin to the liquid flowing inside the tube. The modification in the SSWTHX model improves heat transfer efficiency and reduces the solidification time needed for heat exchange in the paraffin, relative to the SFTHX and STHX models.

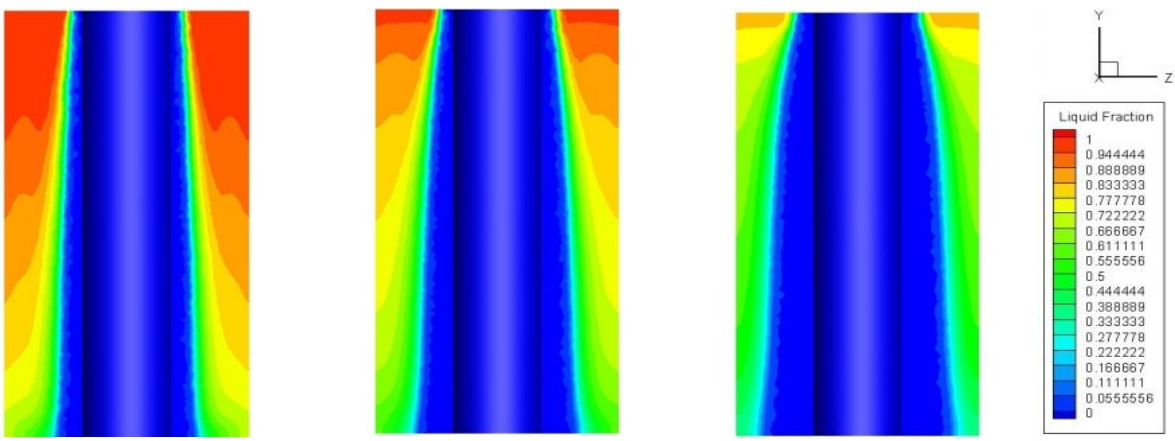

500 (s) 1000 (s) 2000 (s)

(a) STHX Model

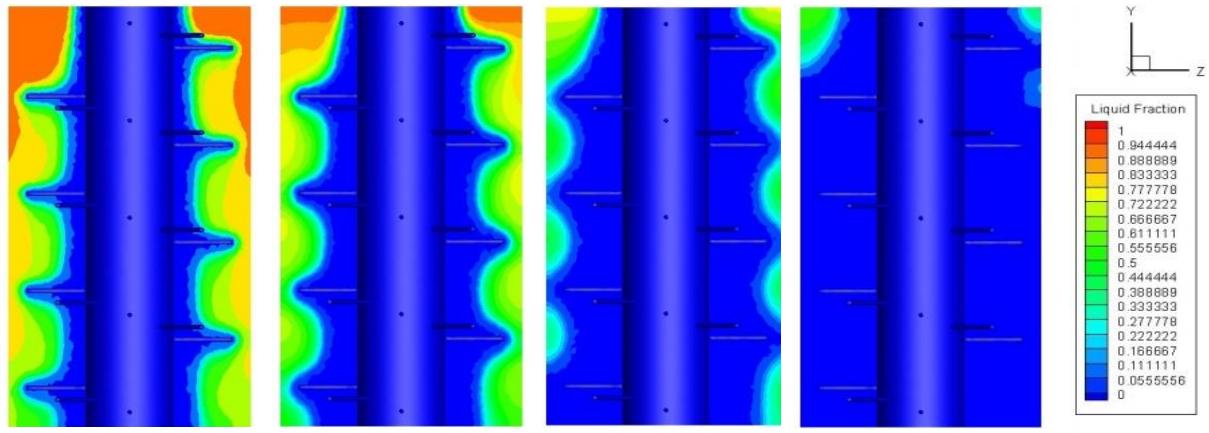

(b) SFTHX Model

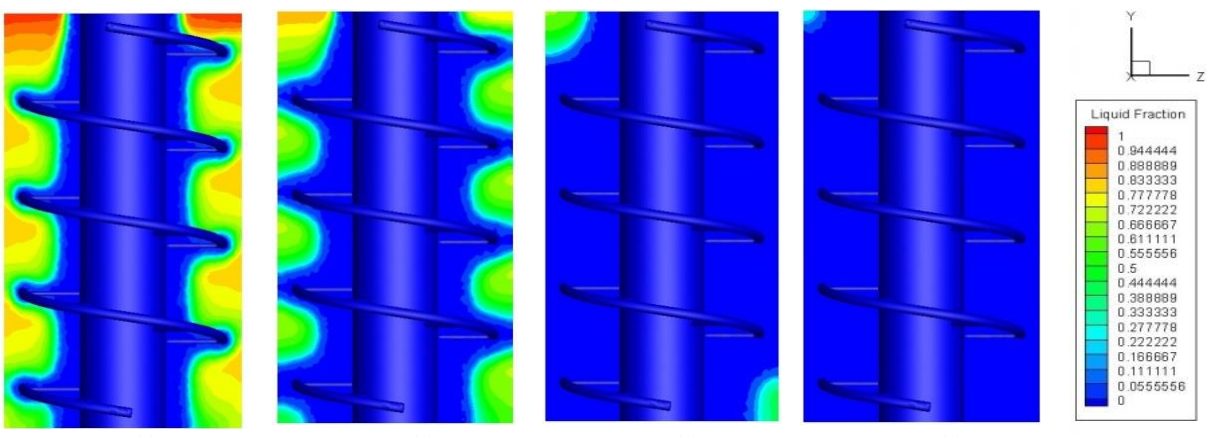

(c) SSWTHX Model

Figure 9. Contours plot of the predicted solidification fraction for models, (a) STHX, (b) SFTHX, (c) SSWTHX

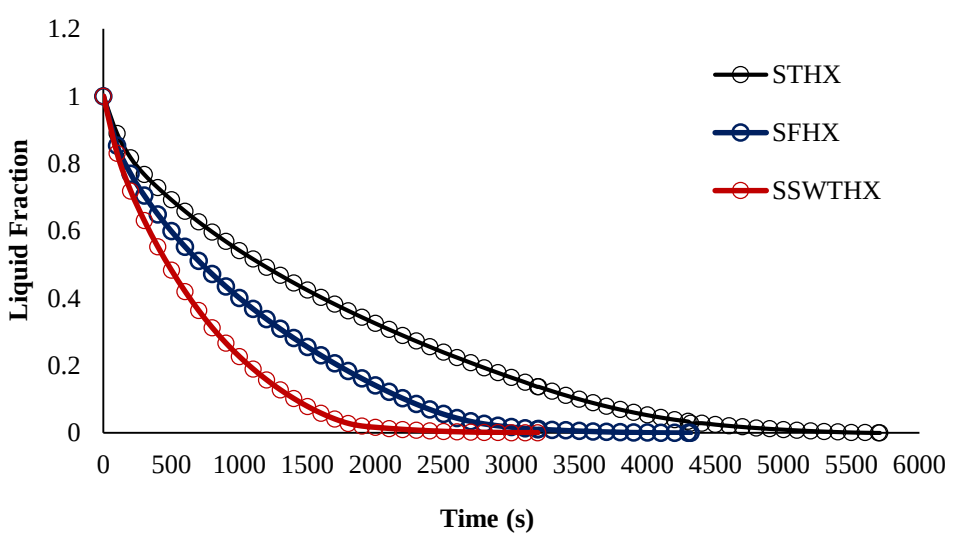

Figure 10. Comparison of the average solid fraction among the proposed models

Another result predicted from the numerical simulation for the three models

is the temperatures in three locations near the pegging, middle, and exit points (T_1, T_2, and T_3) inside the PCM toward the cooling fluid flow direction. Figure 12 shows the behavior of the temperature drop at these locations for the three current models. The results demonstrate that the solidification processes start at the PCM temperature of 340 K, and then decrease gradually with time. The graphs reveal that the temperature drop occurs more rapidly for the three locations of the model with the SSWTHX compared to the SFTHX model and the STHX model. This faster temperature reduction over time highlights the impact of the spiral wire, which ensures a more uniform heat transfer distribution within the paraffin. Additionally, the SFTHX model demonstrates a better temperature gradient distribution than the STHX model.

By averaging the temperatures at the three specified locations for each model and plotting them on a single graph, as shown in Figure 13, it is observed that the paraffin takes 3193 (s) to completely solidify at a temperature of 297.7°C in the SSWTHX model. In contrast, solidification occurs in 4317 seconds for the SFTHX model and 5710 (s) for the STHX model. The decrease in reduction in solidification time demonstrates that the SSWTHX model provides superior performance in heat exchanger enhancement, followed closely by the SFTHX model. Therefore, the presence of fins with the spiral wire in the SSWTHX model improves heat exchange efficiency and accelerates the solidification process.

To validate the numerical results, experimental tests were conducted on the fabricated models which are presented in Figure 8. Figure 14 presents the average temperatures T1, T2, and T3 for both numerical and experimental results during the solidification processes. The results observed that all models follow the same trend for both numerical and experimental results during the solidification process. Based on these results, it can be concluded that the temperature distribution behavior shows strong agreement between numerical simulations and experimental tests, indicating consistent heat transfer behavior between the fluid flowing inside the tube and the PCM during the solidification process.

The observed discrepancy between the numerical and experimental results can be attributed to multiple influential factors. During the numerical analysis, a constant wall temperature was assumed for the copper tube through which the heat transfer fluid flows. This assumption facilitates heat extraction from the paraffin and helps reduce computational costs. Additionally, some numerical assumptions, such as the constant value of the mushy zone, could influence the results. In contrast, the experimental setup involved the use of insulation to minimize the heat loss to the surroundings, whereas the numerical model assumed a perfectly insulated system with no external heat loss. Furthermore, changes in the laboratory environment over time could also contribute to variations in the experimental results.

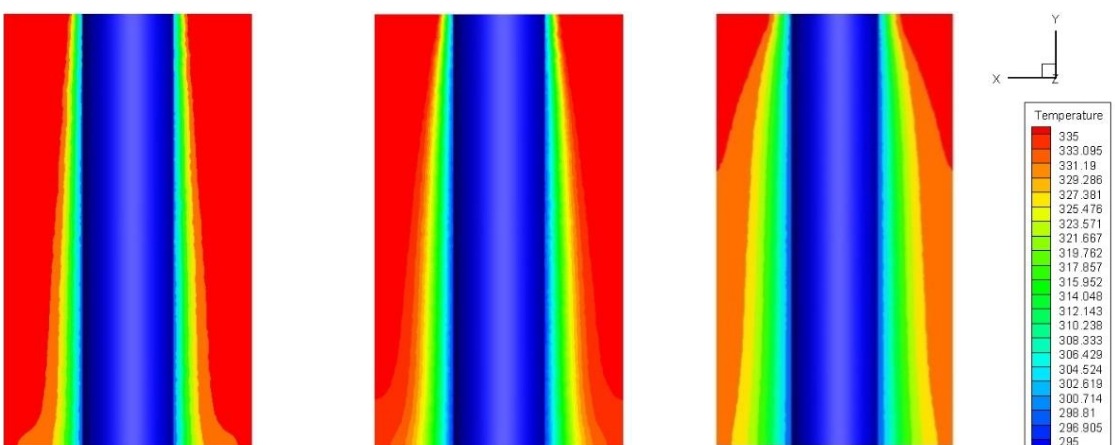

500 (s) 1000 (s) 2000 (s)

(a) STHX Model

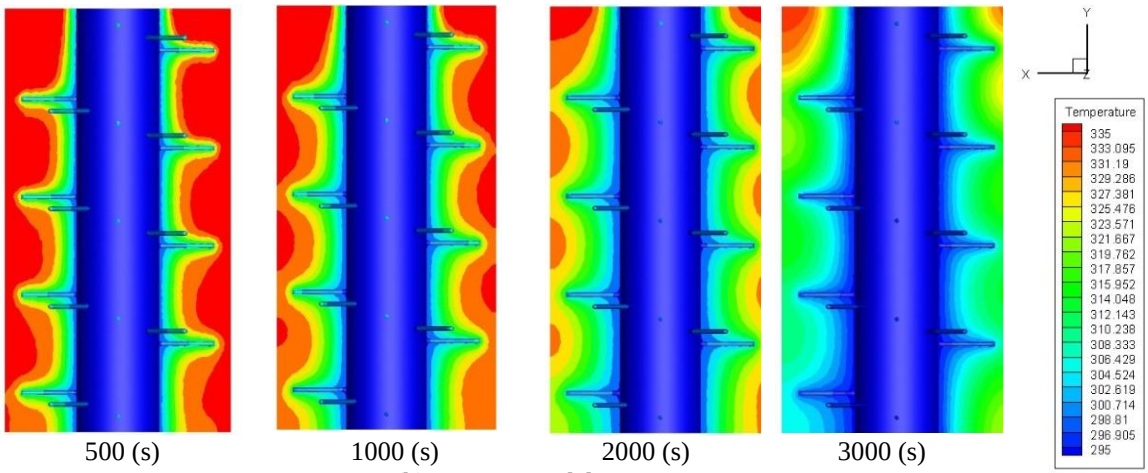

500 (s) 1000 (s) 2000 (s) 3000 (s)

(b) SFTHX Model

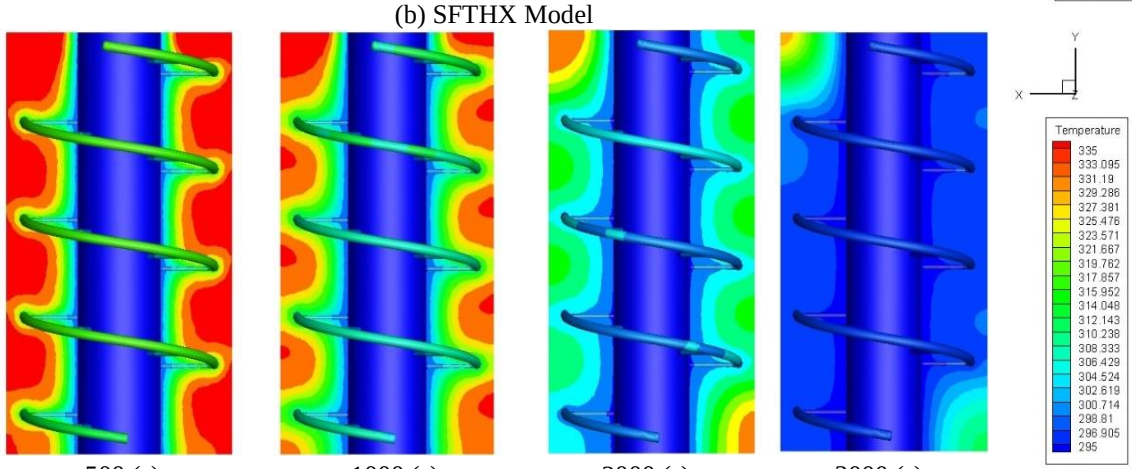

500 (s) 1000 (s) 2000 (s) 3000 (s)

(c) SSWTHX Model

Figure 11. Temperature contours for the current study proposed models. (a) STHX, (b) SFTHX, and (c) SSWTHX

As a further verification of the results compared to those obtained in previous studies, the study of a heat exchanger with spiral configuration is a relatively new one, and hasn't been addressed previously in the authors' earlier research [19] concerning the melting process. Furthermore, the results obtained in the current study are consistent with those of the previous research, as the third heat exchanger model (SSWTHX) demonstrated a significant improvement in heat storage performance compared to previously studied heat exchanger models.

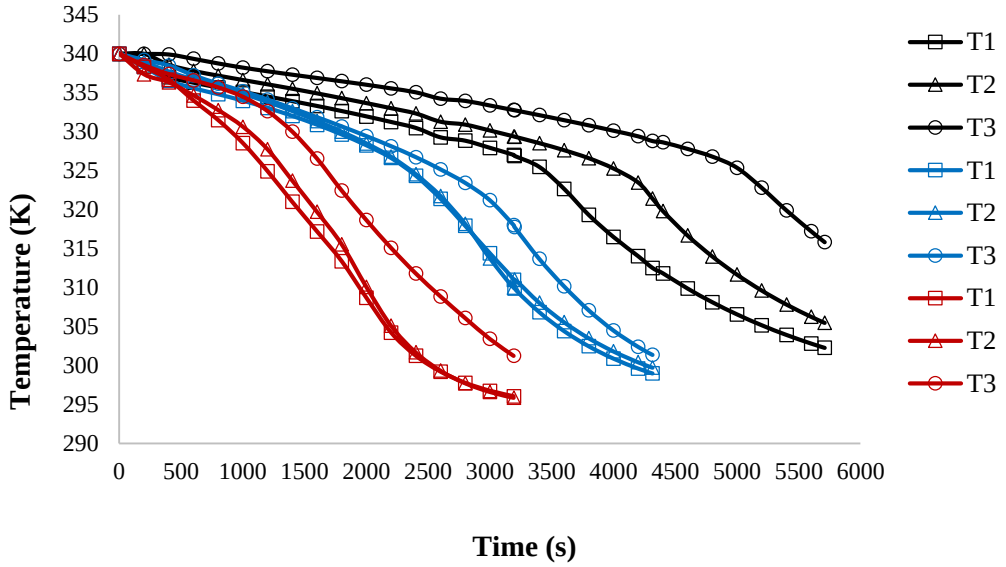

Figure 12. Temperature variation at the locations T1, T2, and T3 for the used models

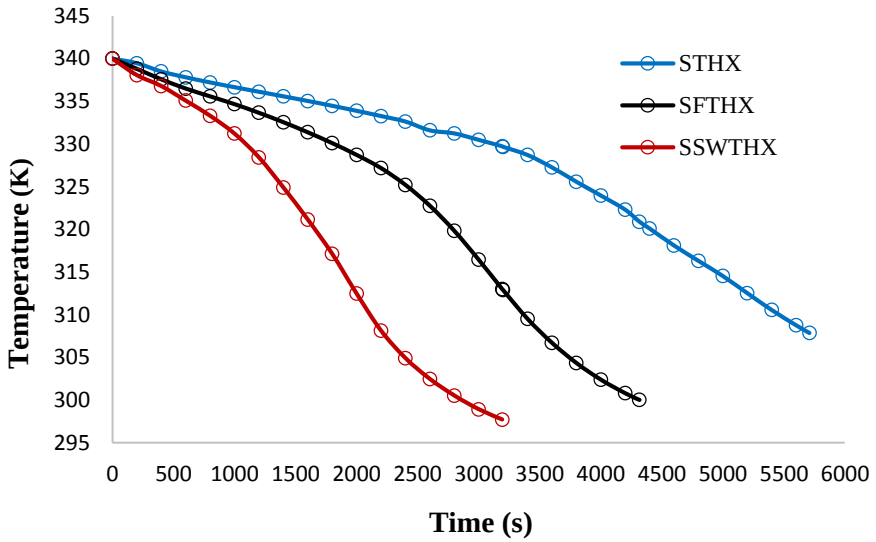

Figure 13. Comparison of average temperatures at measurement points T_1, T_2, and T_3 for the used models

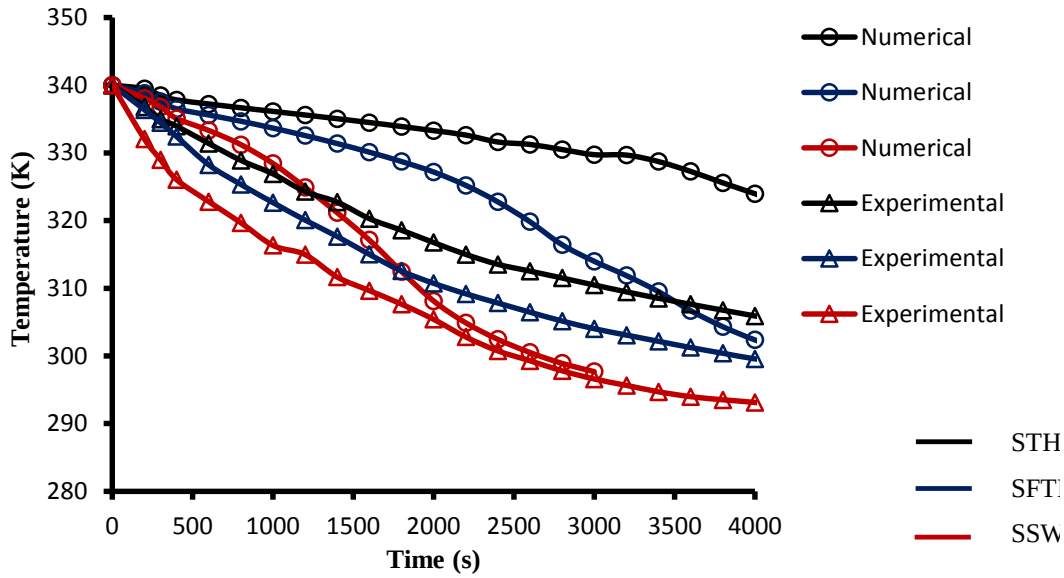

Figure 14. Variation in average temperature between numerical and experimental results at locations T1, T2, and T3 for the used models

5. Estimating the Manufacturing Cost per Unit Length of the Models

An estimated cost analysis of the manufacturing costs per unit length of the models proposed in this study was conducted to assess their manufacturing feasibility. This estimation and evaluation provide a deeper understanding of the balance between improving the heat exchanger's thermal performance and the manufacturing cost. The estimated cost per unit length is approximately 67 $ for the STHX model, 85-90 $ for the SFTHX model, and finally 95-105 for the SSWTHX model. The STHX model is considered a simple model as it only requires preparing the tube with the phase change material. The higher cost for both the pin fins (SFTHX) and the spiral wire with pin fins (SSWTHX) is attributed to the complexity of manufacturing, as well as the welding process, which requires more precision assembly and sufficient manufacturing time. Additionally, the improved models include additional materials. Despite all the manufacturing complexities of the improved models and the added costs, they increase the performance of the heat exchanger and thus improve its thermal efficiency in storing heat in the phase change material acquired from solar energy, and reduce the time required to store this energy.

6. Conclusions

Latent heat storage systems using a heat exchanger play a crucial role in harnessing solar thermal energy by storing it during the daytime and releasing it at night, during cloudy weather, or in the presence of dust, rain, and smoke. This is achieved through the use of phase change materials (PCMs) such as paraffin. This study relied on numerical and experimental investigations to improve the stored energy discharge performance of PCM-based systems during solidification processes. Three models were investigated: featuring pin-fins (SFTHX) and spiral wire wrapped around fins (SSWTHX). They were compared with the third model, a conventional shell and tube heat exchanger (STHX), to evaluate the improvements in thermal performance. From the predicted solidification rate, it was observed that the time reached 2000 seconds; the paraffin had discharged approximately 75% of its stored energy using the STHX model, while 90% of paraffin had solidified when the discharge time reached 3000 seconds for the SFTHX model, and 98% of paraffin had solidified for the SSWTHX model

The numerical results also indicated that the paraffin in the SSWTHX model completely solidified in 3193 seconds, while the SFTHX and STHX models required 4317 seconds and 5710 seconds, respectively, reaching full solidification. This corresponds to performance improvements in the

solidification process of approximately 44% for the SSWTHX model and 25% for the SFTHX model compared to the STHX baseline.

Based on these results, it can be concluded that the temperature distribution behavior exhibits strong agreement between numerical simulations and experimental tests, indicating consistent heat transfer behavior between the fluid flowing inside the tube and the PCM material during the solidification process. Finally, the study confirms strong agreement between the numerical predictions and experimental results, validating the improved performance of the proposed thermal storage system and demonstrating the achievement of the study objective.

In addition it can be drawn from the thermal analysis of the models, an estimation of the economic and manufacturing costs of these models was also conducted. The estimated costs per unit length are $67 for STHX, 85-95 $ for SFTHX, and 95-105 for SSWTHX models, respectively. Despite the increased cost of the improved models, they provided a performance improvement for the process of energy stored in the heat exchanger.

Regarding future work, there are still some research that can be explored, for example, other suitable and less expensive types of phase change materials can also be used. In addition to the integration of nanoparticles with the phase change material to enhance heat transfer between the fluid flowing inside the tube and these materials. On the other way various fin shapes can be developed. Finally, it is possible to design and manufacture a complete system and conduct an actual study for the whole system.

There were limitations to both parts of this work, the numerical simulation and the experimental work. In the simulation, the work was performed in three dimensions, which increased the model's size and simulation time; therefore, this required specialized computer specifications and large memory. While for the experimental part, the limitations lay in the difficulty of manufacturing the models due to a unavilable of sufficient equipment, especially the suitable equipment for welding the fins to the tube, and also forming and welding the spiral wire. Furthermore, there was extensive research required to obtain paraffin wax with suitable properties acceptable for this research.

Numenclature

CFD	Computational Fluid Dynamics
FVM	Finite Volume Method
LHTE	latent heat storage thermal energy storage
HTF	Heat transfer fluid
PCM	Phase change material
PCMs	Phase change materials
STHX	Shell-and-tube heat exchanger
SFTHX	shell-and-finned tube heat exchanger
SSWTHX	Shell and spiral wire-wound on the finned tube heat exchanger
SIMPLE	Semi-implicit method for pressure-linked equation
γ	Thermal expansion coefficient (K^{-1})
T_0	Temperature of the operating (K)
t	Time (s)
V	Velocity (m/s)
μ	Viscosity (Pa.s)
ρ	Density (kg/m^3)
P	Global pressure (Pa)
$\vec{s}$	Momentum sources term (N/m^3)
S_h	Energy sources term (W/m^3)
K	Thermal conductivity (W/m.K)
h	Enthalpy ($kg.m^2/s^2$)
β	Solid fraction to avoid division by zero
A_{mush}	Constant mushy zone adjusted to (10^5 kg/m^3)
$\vec{g}$	Acceleration due to gravity (m/s^2)

References

[1] Hashemian, N. and Noorpoor, A. (2023). Thermo-eco-environmental investigation of a newly developed solar/wind powered multi-generation plant with hydrogen and ammonia production options. Journal of Solar Energy Research, 8(4), 1728–1737. doi:10.22059/jser.2024.374028.1388.

[2] Ismaeel, A.A., Hussein, N.F., Suffer, K.H. and Razlan, Z.M. (2021). Experimental implementation of thermal enhancement performance of air heat exchanger's pipes utilizing unconventional turbulator. EUREKA: Physics and Engineering, (3), 35–44. doi:10.21303/2461-4262.2021.001850.

[3] Abdellatif, H.E., Khan, S.A. and Liu, H. (2025). Thermal optimization of PCM-based storage systems using L-shaped fins: A numerical and RSM-based approach. Energy, 336, 138309. doi:10.1016/j.energy.2025.138309.

[4] Alyousifi, S.O. and Ahmed, M.I. (2026). A comparative study of techno-economic feasibility of grid and hybrid solar energy systems versus government electricity tariff in Duhok. Journal of Solar Energy Research, 10(4), 2657–2671. DOI:10.22059/jser.2026.404772.1661

[5] Hasan, A.A. and Jassim, N.A. (2020). Thermal energy shifting using thermal energy storage with solar assisted system for space cooling application. Al-Nahrain Journal for Engineering Sciences, 23(3), 216–224. http://doi.org/10.29194/NJES.23030216.

[6] Yazdanparast, S.A., Setareh, M. and Basirat Tabrizi, H. (2026). Numerical investigation of melting characteristics of fin-assisted PCM storage system. Discover Mechanical Engineering, 5(1), 14. doi:10.1007/s44245-026-00185-z.

[7] Saleh, H., Abd-Elhady, M. S., Khalil, T., Mansour, N., & Dahlihaus, D. (2026). Fin Optimization of a Rectangular Heat Sink Integrated with Phase Change Materials. Heat Transfer Engineering, p. 1–19. https://doi.org/10.1080/01457632.2026.2649997.

[8] Alma'asfa, S.I., Aziz, M. S. A., Khor C. Y., & Fraige, F. Y. (2025). Thermal management of lithium-ion batteries with fin configurations and PCM. Journal of Thermal Analysis and Calorimetry, 150(16), 12643–12662. doi:10.1007/s10973-025-14515-y.

[9] Afsharpanah, F., Ajarostaghi, S.S.M. and Arıcı, M. (2022). Phase change time reduction in shell-and-tube ice storage system. International Communications in Heat and Mass Transfer, 137, 106281.doi:10.1016/j.icheatmasstransfer.2022.106281.

[10] Hasan, H.A. and Suffer, K.H. (2024). Modeling of shell and tube shapes with annular fins. E3S Web of Conferences. doi:10.1051/e3sconf/202458905004.

[11] Tiari, S., Qiu, S. and Mahdavi, M. (2016). Discharging process of finned heat pipe thermal storage system. Energy Conversion and Management, 118, 426–437. doi:10.1016/j.enconman.2016.04.025.

[12] Tiari, S., Hockins, A. and Shank, K. (2022). Latent heat thermal storage system with annular fins. Journal of Energy Storage, 55, 105603. doi:10.1016/j.est.2022.105603.

[13] Korawan, A. D., Soeparman S., Wijayanti, W., and Widhiyanuriyawan, D. (2017). Numerical and experimental study on paraffin wax melting. Modelling and Simulation in Engineering, 9590214. doi:10.1155/2017/9590214.

[14] Shaeli, M. N., Jalil, J. M., Baccar , M. (2025). Investigation of photovoltaic thermal performance using air jet impingement as cooling system with varying jet diameters and phase change material. Energy and Buildings, 2025. **336**: p. 115596. https://doi.org/10.1016/j.enbuild.2025.115596

[15] Shaeli, M. N., Jalil, J. M., Baccar, M. (2024). Improving the performance of solar photovoltaic thermal cells using jet impingement and phase change materials cooling technology. Renewable Energy, 2024. 227: p. 120536. https://doi.org/10.1016/j.renene.2024.120536

[16] Saleh, E. M. and Hameed, V. M. (2024). New solar parabolic trough collector with PCM. Journal of Energy Storage, 86, Part B, 111403. https://doi.org/10.1016/j.est.2024.111403

[17] Yan, P., Fan, W., Yang, Y., Ding, H., Arshad, A., and Wen, C. (2022). Performance enhancement of phase change materials in triplex-tube latent heat energy storage system using novel fin configurations. Applied Energy, **327**, 120064. https://doi.org/10.1016/j.apenergy.2022.120064.

[18] Fadl, M., Mahon, D. and Eames, P.C. (2021). Thermal performance analysis of compact thermal energy storage unit-An experimental study. International Journal of Heat and Mass Transfer, 2021. **173**: p. 121262. https://doi.org/10.1016/j.ijheatmasstransfer.2021.121262.

[19] Hasan, H.A. and Suffer, K. H. (2023). Thermal performance enhancement of energy storage system using spiral-wired tube heat exchanger. Energy Sources, Part A: Recovery, Utilization, and Environmental Effects, 2023. **45**(3), P. 7280–7293. https://doi.org/10.1080/15567036.2023.2220676.

[20] Modi, N., Wang, X. and Negnevitsky, M. (2023). Experimental investigation of the effects of inclination, fin height, and perforation on the thermal performance of a longitudinal finned latent heat thermal energy storage. Energy, 274, 127327. https://doi.org/10.1016/j.energy.2023.127327

[21] ANSYS Fluent Inc. (2019). Fluent User Guide 19.0.

[22] Patankar, S.V. (1980). Numerical Heat Transfer and Fluid Flow. Taylor and Francis.

[23] Voller, V.R. and Prakash, C. (1987). Fixed grid phase-change model. International Journal of Heat and Mass Transfer, 30(8), 1709–1719. doi:10.1016/0017-9310(87)90317-6.

[24] Al-Abidi, A. A., Mat, S. B., Sopian, K., Sulaiman, M. Y., and Mohammed, A. T. (2013). CFD applications for latent heat storage review. Renewable and Sustainable Energy Reviews, 20, 353–363. doi:10.1016/j.rser.2012.11.079.

[25] Bernardo Buonomo, B., Ercole, D., Manca, O., and Nardini, S. (2016). Thermal Behaviors of Latent Thermal Energy Storage System with PCM and Aluminum Foam. International Journal of Heat Technology, 34, S359–S364. doi:10.18280/ijht.34S224.

[26] Zhang, P., Meng, Z., Zhu, H., Wang, Y., and Peng, S. (2015). Experimental and numerical study of heat transfer characteristics of a paraffin/metal foam composite PCM. Energy Procedia, 2015. **75**: p. 3091–3097. doi: 10.1016/j.egypro.2015.07.637.

[27] Youssef, W., Ge, Y. T., and Tassou, S. A. (2018). CFD modelling development and experimental validation of a phase change material (PCM) heat exchanger with spiral-wired tubes. Energy conversion and management, 2018. 157: p. 498–510. https://doi.org/10.1016/j.enconman.2017.12.036 [28] Hasan, H.A. and Hussain, I.Y. (2018). Theoretical formulation and numerical simulation of thermal performance enhancements for cascade thermal energy storage systems. IOP Conference Series: Materials Science and Engineering. 433, 012043. doi:10.1088/1757-899X/433/1/012043.

[29] Jalil, J.M. and Salih, S.M. (2020). Analysis of Thermal and Insulation Performance of Double-Glazed Window Doped with Paraffin Wax. Engineering and Technology Journal, 2020. **38**(3): p. 383–393. https://doi:10.30684/etj.v38i3A.448

[30] Hasan, H.A. (2025). Nanoparticle-enhanced latent heat storage. Arabian Journal for Science and Engineering, 50(4), 2265–2276. doi:10.1007/s13369-024-09054-x.

[31] Wang, P., Wang , X., Huang, Y., Li, C., Peng, Z., and Din, Y. (2015). Thermal energy charging behaviour of a heat exchange device with a zigzag plate configuration containing multi-phase-change-materials (m-PCMs). Applied energy, 2015. 142: p. 328–336.
https://doi:10.1016/j.apenergy.2014.12.050

[32] Arena, S., Casti, E., Gasia, J., Cabeza, L. F., and Cau, G. (2017). Numerical simulation of a finned-tube LHTES system: influence of the mushy zone constant on the phase change behaviour. Energy Procedia, 2017. 126: p. 517–524. https://doi:10.1016/j. egypro.2017.08.237

[33] Hasan, H.A. and Hassoon, A.S. (2023). Thermal performance investigation of finned latent heat storage of shell- and- tube, shell- and- nozzle, and shell- and- reducer models. Heat Transfer, 2023. 52(7): p. 4755–4773. https://doi.org/10.1002/htj.22906